

## Carbohydrates

## Sulfation Patterns of Saccharides and Heavy Metal Ion Binding

Israel Alshanski,<sup>[a]</sup> Joanna Blaszkiwicz,<sup>[b]</sup> Evgeniy Mervinetsky,<sup>[a]</sup> Jörg Rademann,<sup>\*,[b]</sup> Shlomo Yitzchaik,<sup>\*,[a]</sup> and Mattan Hurevich<sup>\*,[a]</sup>

**Abstract:** Sulfated saccharides are an essential part of extracellular matrices, and they are involved in a large number of interactions. Sulfated saccharide matrices in organisms accumulate heavy metal ions in addition to other essential metal ions. Accumulation of heavy metal ions alters the function of the organisms and cells, resulting in severe and irreversible damage. The effect of the sulfation pattern of saccharides on heavy metal binding preferences is enigmatic because the accessibility to structurally defined sulfated sac-

charides is limited and because standard analytical techniques cannot be used to quantify these interactions. We developed a new strategy that combines enzymatic and chemical synthesis with surface chemistry and label-free electrochemical sensing to study the interactions between well-defined sulfated saccharides and heavy metal ions. By using these tools we showed that the sulfation pattern of hyaluronic acid governs their heavy metal ions binding preferences.

## Introduction

The extracellular matrices (ECM) of higher organisms play vital roles in the signaling, sensing and communication of cells; thus, targeting the ECM lies at the heart of drug and vaccine development.<sup>[1]</sup> However, understanding the specific interactions of each component of the ECM constitutes a major challenge. Since the ECM contains a huge number of different chemical entities that have a variety of interacting partners (i.e., protein-protein, saccharide-protein, and saccharide-saccharide interactions), meeting this challenge requires the development of original analytical approaches and new synthetic strategies. Sulfated saccharides such as glycosaminoglycans (GAG) and carrageenans are major components of the ECM of organisms from animals to algae.<sup>[2,3]</sup> These molecules have a large variety of sulfation patterns that affect their structural properties and biological activities.<sup>[4-6]</sup> Given that sulfated saccharides exist in metal-ion-rich environments, they interact with, absorb, and store a variety of metal ions.<sup>[7-9]</sup> Metal ion binding to saccharides can result in changes of the physical properties and the biological interactions of these saccharides and can lead to the accumulation of both essential and toxic

heavy metal ions.<sup>[10,11]</sup> Previous studies suggested that the interactions of metal ions with sulfated saccharides are dictated by a combination of structural and functional factors.<sup>[12]</sup> These studies claim that cations can form electrostatic interactions with several moieties in the saccharide.<sup>[12]</sup> On the other hand, the interaction between the two is subjected to conformation related effects, which lead to binding preferences and specificity.<sup>[13,14]</sup>

Most heavy metals are found at low concentrations in the natural environment and can interact with sulfated saccharide matrices.<sup>[15]</sup> Cadmium, mercury and lead are present in toxic, sometimes lethal, concentrations in soil, fresh water sources and sea water that are in proximity to industrial infrastructure.<sup>[16-19]</sup> Thus, it is important to monitor the concentrations of these ions and to understand more deeply the factors that govern their accumulation in the ECM of specific tissues and by specific organisms.<sup>[20-22]</sup> It is suggested that sulfated oligosaccharides are used by organisms as protective matrices against heavy metal ion toxicities but over-accumulation of these cations results in diseases and death.<sup>[22,23]</sup>

The effect of sulfation of saccharides on heavy metal binding is largely unknown because it is very difficult to obtain saccharides with defined size and sulfation pattern.<sup>[2,3]</sup> Alternatively, artificial sulfated polymers such as polystyrene sulfonate have been used as replacements for saccharides but these compounds lack the rich structural properties of the native entities.<sup>[24-26]</sup> These shortcomings suggest that well-defined saccharides are required to study the exact effect of sulfation on metal binding properties.<sup>[27]</sup>

Sulfated hyaluronic acids (sHA) are synthetic oligosaccharides derived from hyaluronic acid (HA) that largely resemble native sulfated GAG such as chondroitin, dermatan or heparan sulfate (Figure 1 A and C).<sup>[28-31]</sup> They were used to study protein glycan interactions, for biomedical applications, and they are

[a] I. Alshanski, E. Mervinetsky, Prof. S. Yitzchaik, Dr. M. Hurevich  
Institute of Chemistry and Center for Nanoscience and Nanotechnology  
The Hebrew University of Jerusalem, Safra Campus  
Givat Ram, Jerusalem, 91904 (Israel)  
E-mail: mattan.hurevich@mail.huji.ac.il  
shlomo.yitzchaik@mail.huji.ac.il

[b] J. Blaszkiwicz, Prof. Dr. J. Rademann  
Medicinal Chemistry, Freie Universität Berlin  
Königin-Luise-Strasse 2+4, Berlin, 14195 (Germany)  
E-mail: joerg.rademann@fu-berlin.de

Supporting information and the ORCID identification number(s) for the author(s) of this article can be found under:  
<https://doi.org/10.1002/chem.201901538>

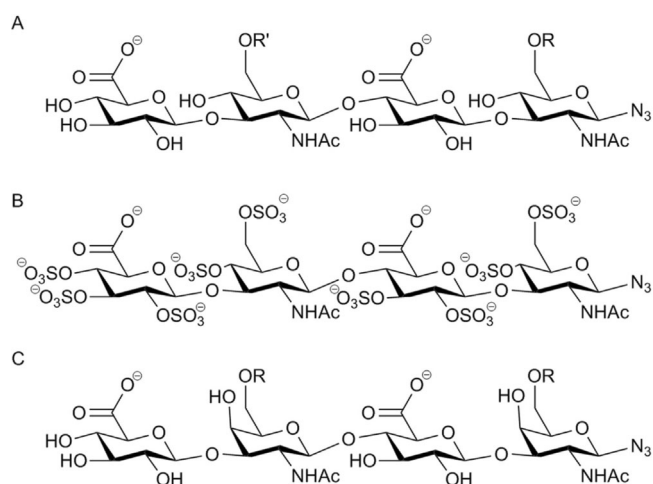


**Figure 1.** Tetrasaccharides with different sulfation patterns. A and B were azide oligohyaluronans used in this study, and C is an example of azide chondroitin sulfate C (CS-C) tetrasaccharide analogue. A) Non-sulfated HA tetrasaccharide (**HA4**)  $R=R'=H$ , mono-sulfated HA tetrasaccharide mixture of  $R=SO_3^-$ ,  $R'=H$  and  $R=H$ ,  $R'=SO_3^-$  (**msHA4**) and di-sulfated HA tetrasaccharide (**dsHA4**)  $R=R'=SO_3^-$ ; B) non-sulfated HA tetrasaccharide (**9sHA4**); C) azide CS-C tetrasaccharide.

well accepted as biologically relevant GAG related models.<sup>[32–35]</sup> sHA have been successfully used to study the interactions with GAG-binding sites of many regulatory proteins and for the design of artificial extracellular matrices with tailored functions.<sup>[36–39]</sup> Recently, we have developed strategies to produce a variety of defined sHA from readily available HA in larger quantities by using a combination of enzymatic and chemical methods.<sup>[40,41]</sup> These defined sHA are attractive tools for the selective detection of heavy metals in polluted environments, to study the molecular aspects involved in the interactions with heavy metals, and finally to elucidate how sulfation patterns effect GAG heavy metal binding preferences.<sup>[42]</sup>

Interactions of peptides, proteins and oligonucleotides with small molecules and metal ions are mostly studied using analytical methods that rely on fluorescence, luminescence, circular dichroism (CD), or absorbance.<sup>[43–46]</sup> These methods are difficult to use for analyzing interactions between saccharides and metal ions because little spectroscopic change arises from such binding.<sup>[47]</sup> Peptides and oligonucleotides are much richer in metal chelating moieties both in the side chains and in the backbone, whereas saccharides contain mainly hydroxyl groups that are weak chelators and are poor in stronger chelating groups.<sup>[48,49]</sup> In addition, saccharide–metal complexes lack characteristic absorbance, and labeling saccharides is synthetically challenging and might interfere with these interactions.

Electrochemical analysis does not rely on absorbance, mass changes or heat transfer and can provide a valuable tool to study interactions between saccharides and heavy metals. Electrochemical impedance spectroscopy (EIS) is a label-free technique that is sensitive to dielectric properties of the interface and surface density variation that results from the interactions of the recognition layer with the analytes.<sup>[50]</sup> EIS of electrodes with biomolecules as recognition element have previously

been used in many biosensors to detect trace amounts of metal ions.<sup>[51–53]</sup>

Here, we develop original tools and strategies that will help to establish the biochemical, pharmaceutical, and medicinal significance of the interactions between sulfated saccharides and heavy metals. We postulate that EIS can be used to study the interactions of sHA with heavy metal ions and to overcome the limitations of the other analytical techniques. In addition, electrochemical characterizations should be able to provide insights into the effect of sulfation pattern of a saccharide on heavy metal binding preferences.

Therefore, we envision a label-free, robust and reproducible system that is capable of detecting low concentrations of heavy metal ions by using well-defined saccharides in a quantitative manner. To achieve this, we will synthesize a series of defined sulfated hyaluronic acid tetrasaccharides with distinctive sulfation patterns functionalized with azide moiety (**sHA4**). Next, we will develop a robust way to covalently anchor the sulfated saccharides to electrodes using the copper-free strain-promoted click reaction to avoid the presence of transition metals in the system.<sup>[54,55]</sup> The surfaces generated by this approach will be characterized by using atomic force microscopy (AFM) contact angle (CA) and ellipsometry. These surfaces will enable us to investigate correlations between sulfation patterns and metal ion binding by using label-free electrochemical techniques, especially, EIS and cyclic voltammetry (CV), and to evaluate the response of different **sHA4** to increasing concentrations of the heavy metal ions,  $Cd^{2+}$ ,  $Hg^{2+}$ , and  $Pb^{2+}$ . In addition, metal ion binding to the surfaces will be verified by X-ray photoelectron spectroscopy (XPS). For comparison, we will investigate isothermal titration calorimetry (ITC) as another label-free method to analyze metal ion interactions with **sHA4** in solution.<sup>[56–58]</sup> As a result, we will be able to provide novel insights into metal ion binding of defined sulfated GAG.

## Results and Discussion

### Synthesis of HA tetrasaccharides

HA is a linear polysaccharide made from a disaccharide repeating unit of *N*-acetylglucosamine (GlcNAc) and glucuronic acid (GlcA). Polymeric HA is natively non-sulfated, but chemically sulfated HA serves as an attractive model for native GAG because they are easier to obtain in large quantities and high purity. To investigate metal ion interactions of sulfated HA with metal ions,  $\beta$ -azide HA tetrasaccharides with defined size and sulfation pattern were obtained by using a combination of chemical and chemoenzymatic protocols (Figure 1, and the Supporting Information).<sup>[59,60]</sup>

For partial sulfation, **HA4** was treated with six equivalents of sulfur trioxide pyridine complex in *N,N*-dimethylformamide (DMF). Elution of the reaction mixture over a weak anion exchanger with NaCl furnished the mono-*O*-6-sulfo-tetrahyaluronan azide (**msHA4**) and di-*O*-6-sulfo-tetrahyaluronan azide (**dsHA4**) in 32% and 35% yield, respectively, after desalting. The following set of HA tetrasaccharide-azides with various sulfation patterns were used to study the metal ions interactions.

**HA4** was used as a non-sulfated control, whereas **msHA4** has only one sulfate group and **dsHA4** has two. **msHA4** is a mixture of 60% of **6SHA4** where the sulfate is on GlcNAc-1 and 40% of **6'SHA4** with the sulfate on GlcNAc-3. As a second control, nonasulfated **HA4 (9sHA4)** was used.

### Surface modification and characterization

To prepare a sensor in which the sulfated saccharides are covalently linked to the surface, a strategy based on the bioorthogonal click chemistry was chosen. To avoid any metal-mediated process, we relied on copper-free, strain-promoted click reaction of azido **sHA4** with a dibenzocyclooctyne (DBCO) moiety that was previously anchored to a modified oxide surface (Figure 2).<sup>[61,62]</sup>

To characterize the system and the assembly process, all fabrication steps were performed on silicon wafer prior to electrode preparation. Each assembly step was analyzed by three different methods: spectroscopic ellipsometry, wettability by contact angle (CA), and atomic force microscopy (AFM). In the first step, the silicon wafer was oxidized by using a reported procedure.<sup>[63,64]</sup> The silicon-dioxide layer activation resulted in a thickness of 17.9 Å, root mean square (RMS) roughness of 0.67 nm and contact angle lower than 20°. The resulting oxide layer was reacted with (3-aminopropyl)triethoxysilane (APTES) and an additional smoother and more hydrophobic layer was formed with a thickness of 6.3 Å, a roughness of 0.17 nm, and a CA of 56°.

Coupling of dibenzocyclooctyne-*N*-hydroxysuccinimidyl ester (DBCO-NHS) to the amine modified surface resulted in addition

of a smooth and hydrophobic layer with thickness of 6.5 Å and CA of 67°. On the last assembly step, the azide functionalized **msHA4** was attached to the DBCO moiety on the surface by using a copper-free click reaction to eliminate exposure to transition-metal ions that might form complexes with the saccharide.<sup>[62]</sup> This step required only the incubation of the azide saccharides with DBCO functionalized surface in buffer solution without the addition of any metal catalyst (detailed procedure described in the experimental). The thickness in this step was increased by 2.8 Å and the CA decreased to 50° with no change to the roughness. The observed CA trends in all of the assembly steps correlates with the expected change in the surface hydrophobicity. The ellipsometric measurements of the layer thickness was compared to the value calculated based on bond lengths in the extended geometry. The thickness measurements of all steps correlate with the longitudinal axis of the molecule in perpendicular alignment to the surface. The thickness measured following the tetrasaccharide assembly step was lower than the calculated one, thus suggesting that the **sHA** layer is aligned parallel to the surface.

X-ray photoelectron spectroscopy (XPS) analysis was used to determine the presence of distinctive atomic features of the modified silicon wafers. The XPS measurements of **msHA4** modified silicon wafer show a binding energy (BE) peak, at 230 eV (S2s), that correlates with the presence of a sulfate group; this confirms the attachment of the sulfated HA to the modified surface (see the Supporting Information). The analysis of the assembly steps on the silicon wafer indicates that the same protocol can be used to prepare sulfated saccharide-based electrodes. The XPS analysis, in addition to the other

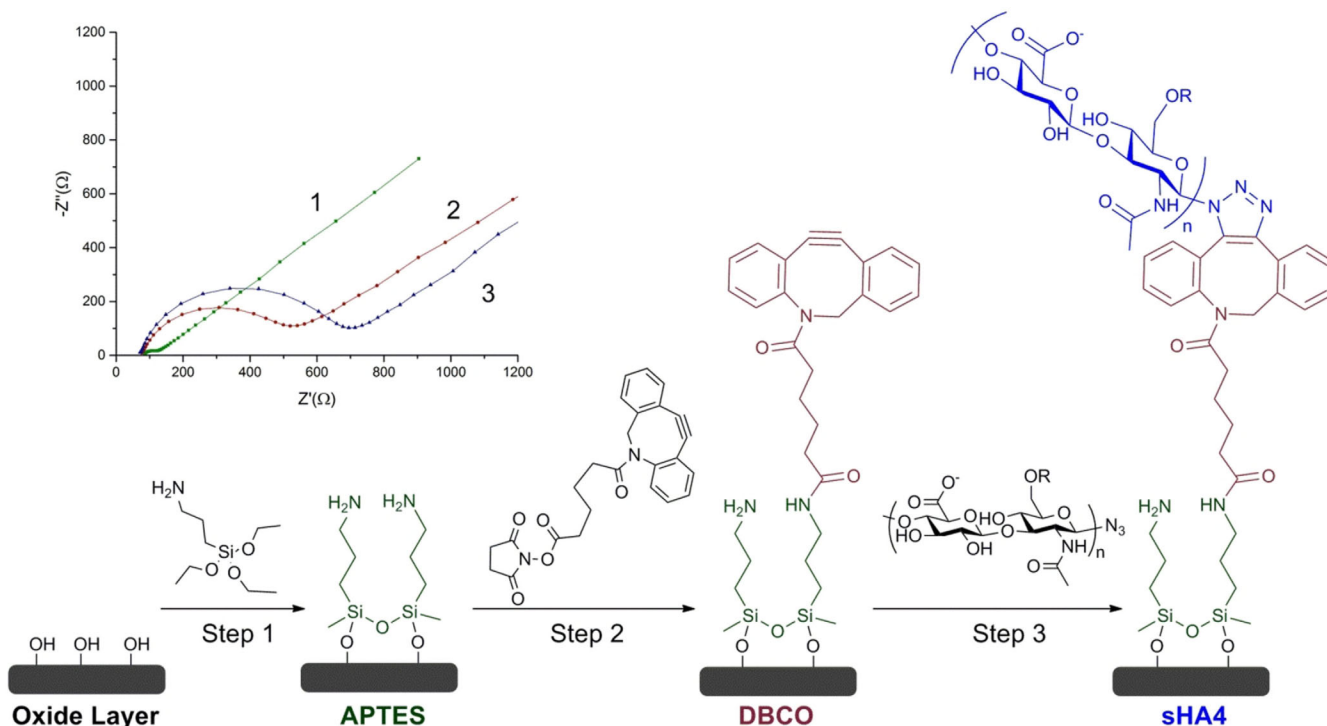


**Figure 2.** HA attachment to GCE surface or silicon wafers, modified with DBCO by copper-free click reaction to form **HA4-GCE**, **msHA4-GCE**, **dsHA4-GCE** and **9sHA4-GCE**. Insert: EIS measurements after APTES assembly (step 1), DBCO coupling (step 2), and HA click coupling represented by green, red, and blue Nyquist plots in the insert, respectively.

methods, confirms the robustness of the system. The XPS show that the molecular features associated with the functional groups, especially the sulfate, of **sHA4** are kept intact after all fabrication steps have been performed.

### Preparation of HA4-GCE electrodes

The electrodes were prepared by modifying an oxidized glassy carbon electrode (GCE) by following the same procedure used for the preparation of silicon wafers (Figure 2). All synthetic modification steps on the GCE were monitored by EIS analysis (see the Supporting Information). In all steps the EIS analysis showed an increase in the resistance of the surface to ferricyanide-ferrocyanide redox couple transport through the layer (Figure 2 insert and the Supporting Information). The preparation protocol was reproducible and the assembly of each of the **HA4** saccharides on the GCE resulted in very similar surface density. This enabled us to further evaluate the response of the saccharide functionalized electrodes to heavy metal ions.

### Impedimetric response to heavy metal ions binding

After the preparation of the saccharide functionalized electrodes, **HA4-GCE**, **msHA4-GCE**, and **dsHA4-GCE**, they were exposed to increasing concentrations of  $\text{Cd}^{2+}$ ,  $\text{Pb}^{2+}$ , and  $\text{Hg}^{2+}$ , and the response was evaluated using EIS. The measured values are shown by Nyquist plot and fitted to the Randles equivalent electrical circuit (see the Supporting Information) extracting the resistance and the capacitance components of the system. To quantify the response to the metal ions, the charge-transfer resistance ( $R_{\text{CT}}$ ) was normalized by dividing the  $R_{\text{CT}}$  value after exposure to heavy metal ions by the  $R_{\text{CT}}$  value before exposure.

When **HA4-GCE**, **dsHA4-GCE** and **msHA4-GCE** were exposed to increasing concentration of mercury ions, only the latter showed a significant increase in the normalized  $R_{\text{CT}}$  value and a negligible decrease in capacitance in the range of 0.1 to 100 nM  $\text{Hg}^{2+}$  (Figure 3 A and B). This suggests that the interaction of **msHA4-GCE** with mercury ions results in substantial change in surface density that is translated to an increase in the impedance. These results show that the interaction of

**msHA4**, which have only one sulfate, with mercury ions is stronger than that of the other HA analogues.

We also evaluated the response of all three tetrasaccharides to lead and cadmium ions over the same range of concentrations (see the Supporting Information). To simplify the analysis, we compared the EIS response of the three **GCE-HA** toward a 100 nM concentration of each of the heavy metal ions since it correlates with the overall dose response trends (Figure 3 C).

**msHA4-GCE** showed some response to lead ions in this concentration region, although much less than to mercury; **HA4-GCE** and **dsHA4-GCE** showed no response to lead. Interestingly, we see a slight increase in the normalized  $R_{\text{CT}}$  of **dsHA4-GCE** as response to  $\text{Cd}^{2+}$  in that concentration range. The EIS results also show that neither **msHA4-GCE** nor **HA4-GCE** respond to the presence of cadmium ions. We also performed EIS studies of a nonsulfated hyaluronan tetrasaccharide analogue (**9sHA4**) (see the Supporting Information). However, this analogue showed no specific response to these metal-ions or any monotonic tendency via dose response (see the Supporting Information). The results of the EIS screening described above suggest that the metal binding is sulfation pattern dependent. This study also demonstrates that polysulfation of a substrate, as used in other materials, is not the appropriate way to achieve metal ion selectivity and sensitivity using oligosaccharide. This supports our hypothesis that the pattern of sulfation and not the number of sulfate groups is the crucial factor for metal ion affinity.

The EIS studies prove that the **HA4-GCE** system is applicable to all saccharides in the library and can be used to detect low concentrations of heavy metal ions. Furthermore, the system is reproducible enough to establish reliably the correlation between the sulfation pattern and heavy metal ions preferences.

### Voltammetric response to heavy metal ions binding

To confirm and quantify the ions binding on the **HA-GCE** surface, cyclic voltammetry (CV) was performed on **HA4-GCE**, **msHA4-GCE**, and **dsHA4-GCE** after exposure to 100 nM concentration of  $\text{Cd}^{2+}$ ,  $\text{Pb}^{2+}$ , or  $\text{Hg}^{2+}$ . CV analysis for **HA4-GCE**, **msHA4-GCE**, and **dsHA4-GCE** after exposure to mercury showed two main differences (Figure 4 A). First, the quantity of

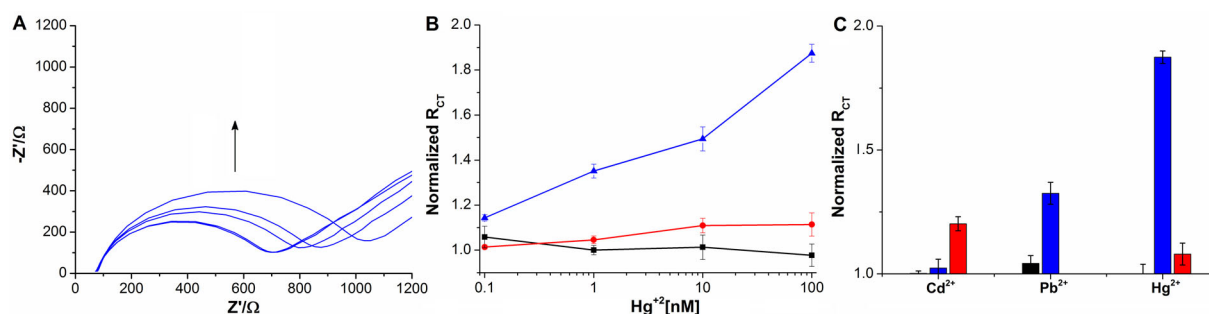


**Figure 3.** Impedimetric response of **HA-GCE** to heavy metal ions. A) **msHA4-GCE** in response to increasing concentrations of  $\text{Hg}^{2+}$  from 0.1 nM to 100 nM represented by Nyquist plots overlay; B) dose-response of different **HA-GCE** to increasing concentrations of  $\text{Hg}^{2+}$  from 0.1 nM to 100 nM ( $N=3$ ); and C) response of different **HA-GCE** to 100 nM concentrations of  $\text{Cd}^{2+}$ ,  $\text{Pb}^{2+}$  and  $\text{Hg}^{2+}$  ( $N=3$ ). Black describes **HA4-GCE**, blue describes **msHA4-GCE** and red describes **dsHA4-GCE**.

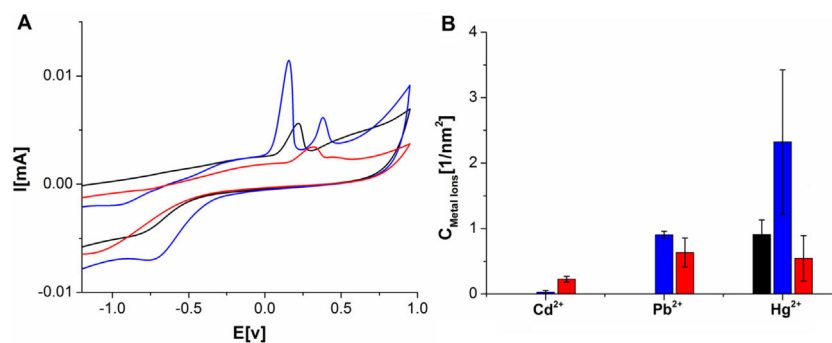


**Figure 4.** CV response of the three tetrasaccharides to: 100 nM Hg<sup>2+</sup> (A) and to 100 nM concentrations of Cd<sup>2+</sup>, Pb<sup>2+</sup>, and Hg<sup>2+</sup> presented as metal ion per nanometer square ( $N=3$ ) (B). Black describes **HA4**, blue describes **msHA4** and red describes **dsHA4**. The real concentration of different metal ions was calculated from the oxidation peak and is presented as metal ion per nanometer square ( $N=3$ ).

ions detected depends on the sulfation pattern, with a clear preference of mercury to the monosulfated functionalized GCE. Second, there are variations in the mercury oxidation potential shifts indicating that different complexes are formed. We assume that the two peaks for **msHA4-GCE** originate either from the formation of two distinctive mercury-HA complexes or from the presence of two oxidation states.<sup>[65]</sup> CV analysis of all three **HA-GCE** after exposure to lead and cadmium also showed differences in the quantity of ions detected on each of the three sulfated HA-GCEs (Figure 4B). Lead was detected on **msHA4-GCE** and **dsHA4-GCE**, albeit in much lower quantity compared to mercury, but not on **HA4-GCE**. We could detect only small amounts of cadmium on **msHA4-GCE** and **dsHA4-GCE** while none was detected on **HA4-GCE**. Similar to mercury, there were shifts in oxidation potential of lead between the differently sulfated saccharides (see the Supporting Information). We assume that these changes in the oxidation potential may result from a different stabilization of lead complexes.<sup>[65]</sup>

CV proved to be a valuable additional tool with which to further decipher sugar metal interaction variances. First, the CV analysis confirmed the presence of the metal ions on the sulfated HA functionalized electrodes. Second and equally important, it allowed us to determine the number of ions on the surface and approximate ratio of metal ions to saccharides.

Assuming homogenous and full coverage, the ratio of saccharide ligand varies from one metal ion per four saccharides, in the case of Cd<sup>2+</sup> and **dsHA4**, to two metal ions per saccharide, in the case of Hg<sup>2+</sup> and **msHA4**. Third, it demonstrated that the sulfation pattern also affects the oxidation potential, thus implying that there is a variation in the type of complex formed in each case.

#### XPS analysis of **msHA4** after exposure to heavy metal ions

XPS was performed on silicon wafer that was covalently attached to **msHA4** to further verify the presence of metal ions on the surface. The XPS analysis clearly indicated the presence of mercury ions (Hg 4f, BE = 101 eV) on surfaces and the absence of cadmium (Cd 3d, BE = 405 eV) as expected from our electrochemical studies. Given that the inner electron energy

for lead is at the same region as the Si plasmon, we used glass slides functionalized with **msHA4** and verified the presence of lead ions (Pb 4f, BE = 138 eV) on this surface (see the Supporting Information). The XPS analysis shows that the heavy ions are complexed and not free, which is in line with the CV results. This provides clear indication that the changes in measured EIS results from complexation of the metal with the tetrasaccharides on the surface.

#### Sulfation pattern effect on heavy metal binding

EIS and CV are complementary analytical methods and, in combination, provide additional insight on the system. EIS is very sensitive to changes in the tetrasaccharides packing properties caused by the metal ion binding, whereas CV measures directly the amount of the metal ions on the surface and their oxidative state. EIS show that mercury changes mostly the surface properties, mainly packing density, of **msHA4-GCE** but not of **HA4-GCE** and **dsHA4-GCE**. CV indicates that mercury is present in all three HA models but show that the quantity of the ion (2.2 nm<sup>-2</sup>) on **msHA4-GCE** is much larger than on the other two (0.9 nm<sup>-2</sup> and 0.5 nm<sup>-2</sup> for **HA4-GCE** and **dsHA4-GCE**, respectively). This observation is in correlation with our EIS results. There are shifts in the oxidation potential of mercury on the three **GCE-HA**. In addition, there are peaks observed in the response of **msHA4-GCE** to mercury. Given that oxidation potential depends on the ability of the ligand to withdraw electrons,<sup>[65]</sup> we assume that there are variations in the type of the complex formed between the ion and the sulfated saccharides. The presence of two peaks for **msHA4** can also be correlated to two oxidation potentials of Hg<sup>1+</sup> to Hg<sup>2+</sup> (+0.91) or Hg<sup>0</sup> to Hg<sup>2+</sup> (+0.85).<sup>[65]</sup> The significant response of **msHA4** to mercury compared with the other systems suggests that the affinity between the two leads to considerable amount of ions on the surface, which, in turn, results in substantial conformational changes of the surface-bound saccharides thus forming a denser monolayer packing. In the case of cadmium, the two methods show slight preference to **dsHA4** over the other two analogues. However, the amount of cadmium ions on **dsHA4** (0.2 nm<sup>-2</sup>) is much lower than that of mercury on **msHA4** (2.2 nm<sup>-2</sup>), indicating a weaker affinity, which is in line with the

relatively minor change in surface density. The response of **msHA4** to lead can be detected both by CV and EIS and results in a considerable surface density change compared with the other saccharides.

The nonsulfated control **9sHA4-GCE** showed only minor response to mercury and none to the other metals in CV analysis and produced a response with high fluctuations by EIS. While there was a clear correlation between the presence and quantity of metal ions (CV) and the surface density changes (EIS) in some cases, for example **msHA4**, in other cases the presence of metal ion complexes did not change the surface density. This indicates that the presence of metal ion complex on the surface does not always lead to a change in the density of the layer. We assume that these differences might originate from variations in oligosaccharide surface number density.<sup>[66]</sup>

The thermodynamics of the interaction of heavy metal ions with the saccharides in solution were investigated by isothermal titration calorimetry (ITC) (see Supporting Information, Figure S37). A solution of  $\text{HgCl}_2$  (500  $\mu\text{M}$ ) in phosphate buffer (8 mM) was titrated in droplets into a solution of **msHA4** (50  $\mu\text{M}$ ) in the same buffer (Figure S37a). For background control, the  $\text{HgCl}_2$  solution was titrated into the same buffer without the monosulfated tetrasaccharide (Figure S37b). In both experiments significant and very similar positive enthalpic contributions were observed, indicating a strongly endothermic process that was dominated by the thermodynamic effects of dilution of the mercury salt solution and not by binding of metal ions to the carbohydrate.

Our studies showed that although all the tetrasaccharides have the same monosaccharide sequence and exactly the same carboxylate and amide metal chelating groups,<sup>[67]</sup> their distinctive affinity and mode of interaction with metal ions are dictated by the sulfation pattern. Furthermore, we clearly observed that a large number of sulfate groups interfere with the chelation ability. This proves that simply "loading" a glycan with sulfates does not necessarily provide preference to metal ions and that the pattern is indeed crucial. It is likely that the sulfation effect on metal binding preference results from a combination of inter- and intra-molecular interactions, electrostatic attraction or repulsion and conformational differences. The effect of sulfation on the conformation of furanosides and GAG was previously reported.<sup>[68,69]</sup> It shows that sulfation alters the conformation of saccharides already on the monosaccharide level. It is reasonable to conclude that sulfation will induce significant conformational changes also on the oligo- and poly-saccharide level that can result in modulation of the affinity toward metal ions. A more profound analysis will be required to elucidate the exact contribution of sulfation to electrostatic and conformational changes of oligosaccharides that leads to the observed heavy metal ion preferences. Our sensors provide us with valuable hints regarding the effect of sulfation on metal binding preferences that adds to the current knowledge on the interaction of sulfated saccharides with their environment.<sup>[32,34]</sup> Our results suggest that the effect of sulfation on the metal binding cannot be simplified merely to the number of sulfate groups. The results indicate that the system is not a simple ion-exchanger but that it is more com-

plex and that the distinctive sulfation pattern of saccharides is crucial for modulating the metal-binding affinities, perhaps through the formation of a secondary coordination sphere.

## Conclusions

We have described a label-free system that can be used to elucidate the interactions of saccharides with heavy metals. A robust synthetic method was developed to anchor small and well-defined sulfated saccharides to the electrode surface via a series of covalent linkages. The method was mild enough so that all the molecular features of the saccharides were kept intact during the monolayer assembly process and robust enough to enable us to characterize the heavy metal ions interaction with the saccharides using various analytical methods. Our studies emphasize the importance of using homogenous saccharides with a known size and sulfation pattern to unravel the unique effect of sulfation on metal interaction preferences. This work proves that label-free EIS and CV provide quantitative analysis of saccharide-metal interactions which are otherwise much harder to elucidate. It also highlights the principle that using homogenous saccharide rather than mixtures can be very attractive for producing selective and sensitive sensors. Considering the large body of evidence that connects the accumulation of heavy metal ions in sulfated-saccharide-rich matrices with alterations in the function and chemical composition of cells, small organisms and brain tissues of high organisms, these events are clearly understudied. We think that the interactions of saccharides with metal ions, especially heavy metal ones, might be governed by sulfation patterns rather than by only the core glycan. These interactions have to be further evaluated to provide a more comprehensive correlation. Studies using a larger set of sulfated saccharides in addition to using analytical tools such as NMR analysis will provide a deeper insight into the mechanism of these interactions and will offer a more accurate picture of the behavior of ECM and saccharide matrices in heavy-metal-rich environments.

## Experimental Section

### Materials

All reagents were of commercial grade (purchased from Sigma-Aldrich, Merck and Alfa Aesar) and were used as received. DBCO-NHS ester was purchased from lumiprobe LTD. For the electrochemical measurements, the trace selective salts, cadmium chloride, mercury(II) nitrate monohydrate, and lead(II) acetate trihydrate purchased from Merck were used. **sHA4** were prepared by following published procedures, synthetic protocols and spectroscopic data are added in the Supporting Information.

### GCE surface modifications and the preparation of HA-GCE

GCE electrodes were manually polished on a micro-cloth pad with de-agglomerated alumina suspension with particle size of 0.05 mm and washed with triple distilled water (TDW). The GCE was activated in a solution of potassium hydroxide 1% w/w in TDW for 40 min at 22 °C, washed with TDW and dried with nitrogen flow.<sup>[62]</sup>

GCE were dipped into 1% 3-aminopropyltriethoxysilane (APTES) in EtOH solution for 40 min at 22 °C washed with EtOH and dried. The electrodes were then placed in an incubator at 45 °C for curing for 2 h, then immersed in a solution of 1 mg mL<sup>-1</sup> dibenzocyclooctyne-*N*-hydroxysuccinimidyl ester (DBCO-NHS, Lumiprobe) in EtOH for 6 h at 22 °C and later washed with EtOH. The DBCO functionalized electrodes were dipped into a solution of 0.1 mg mL<sup>-1</sup> sHA4 in 50 mM ammonium acetate buffer (AA) with pH 6.7 and were incubated for 15 h at 22 °C. After the exposure, the electrodes were washed with AA and measured with EIS. The sHA4 functionalized electrodes were stabilized in AA buffer for 2 h before exposing them to metal ion buffer solutions.

### Silicon wafers modification and exposure to heavy metal ions

Detailed description of the preparation and characterization of silicon wafer functionalized with HA4 can be found in the Supporting Information.

### EIS studies following the exposure of sHA4-GCE to heavy metal ions

sHA4-GCE were exposed to solutions with increasing concentrations (0.1 nM to 1 μM) of lead acetate, cadmium chloride, and mercury nitrate in 50 mM AA buffer at pH 6.7 for 10 min. After the exposure the electrodes were washed with buffer and measured by EIS technique.

### Electrochemical analysis

Electrochemical impedance spectroscopy was performed with ferricyanide-ferrocyanide redox couple with a bio-logic SAS sp-300 potentiostat on modified glassy carbon electrode (GCE). The system was a three-electrode standard electrochemical cell that contained three electrodes in impedance, the three electrodes used in the measurements were: Ag/AgCl (in 3 M KCl) as reference electrode (RE), Pt as counter electrode (CE) and GCE with 3 mm diameter as working electrode (WE). The solution for impedance measurements contained 5 mM Ferro/Ferri redox active couple, 100 mM potassium chloride and 50 mM ammonium acetate buffer with pH 6.7.<sup>[52]</sup>

### Electrochemical impedance spectroscopy (EIS) parameters and Nyquist plot

All measurements were conducted by applying AC potential. Nyquist plots were fitted to equivalent circuit  $R_s[(R_{CT}|W)|C]$  for clean electrode, where  $R_s$  is resistance of the solution,  $R_{CT}$  charge-transfer resistance of the layer,  $C$  is the capacitance and  $W$  is Warburg diffusion element. Electrodes that contain organic layers were fitted with the circuit  $R_s[(R_{CT}|W)|Q]$ , where  $Q$  is constant phase element, that describes a non-ideal capacitor.<sup>[52,62]</sup>

### Cyclic voltammetry (CV) parameters and metal concentration calculation

CV measurements were conducted with sHA4 modified electrodes before and after exposure to 100 nM metal ion in 50 mM AA buffer solution for 10 min. The measurements were conducted from a potential of -2 V to a potential of 1 V at a scan rate of 0.1 V s<sup>-1</sup> in a solution of 50 mM AA buffer at pH 6.7 and 0.1 M of KCl. The total charge was calculated from peak integration with the EC-Lab program. The concentrations of metal ions were calculated from  $M^{2+} = (q \times C) / (A \times 2)$ , where  $M^{2+}$  is the amount of metal ions,  $q$  is the

charge transfer,  $C$  is the coulomb constant and  $A$  is the area of the electrode.

### Isothermal titration calorimetry (ITC)

All ITC measurements were carried out with a Microcal PEAQ-ITC calorimeter (Microcal, Malvern Panalytical, Malvern, GB) at 25 °C. For each titration, 19 to 25 injections of 2.0 and 1.5 μL of titrant, respectively, were conducted at 180 s intervals, while stirring at 750 rpm. Both the titrants and the sample cell solutions were prepared in the same phosphate buffer (8 mM NaH<sub>2</sub>PO<sub>4</sub>·2H<sub>2</sub>O, 2 mM KCl, 0.1% Triton X-100, pH 7.5) to ensure a reasonable baseline and control for all experiments. Two ITC experiments were performed using the following solutions: In experiment 1, (see Supporting Information, Figure S37a), a solution of 500 μM HgCl<sub>2</sub> in the same buffer. In experiment 2, (background control experiment, Figure S37b), the solution of HgCl<sub>2</sub> (500 μM) was added dropwise (1.5 or 2.0 μL per droplet) to the buffer solution without the monosulfated tetrasaccharide msHA4. Subtraction of the recorded heat flow for each droplet of the control experiment from the thermogram of the first experiment was conducted using the point-by-point subtraction mode of the Microcal software.

### Acknowledgements

S.Y. is the Benjamin H. Birstein Chair in Chemistry. The authors would like to thank RECORD-IT project. This project has received funding from the European Union's Horizon 2020 research and innovation program under grant agreement No. 664786. J.R. and J.B. acknowledge support of this work by the Deutsche Forschungsgemeinschaft (DFG) by funding the collaborative research center SFB-TR67 (Functional biomaterials for controlling healing processes of bone and skin, project A8). The authors would like to thank Shahar Dery and Dr. Vitaly Gutkin for their help with the analysis.

### Conflict of interest

The authors declare no conflict of interest.

**Keywords:** analytical methods · carbohydrates · extracellular matrices · surface chemistry · trace analysis

- [1] A. Jeney, *Onco. Targets. Ther.* **2015**, *8*, 1387–1398.
- [2] V. L. Campo, D. F. Kawano, D. B. da Silva, I. Carvalho, *Carbohydr. Polym.* **2009**, *77*, 167–180.
- [3] E. Ruoslahti, *Glycobiology* **1996**, *6*, 489–492.
- [4] B. E. Stopschinski, B. B. Holmes, G. M. Miller, V. A. Manon, J. Vaquer-Alicea, W. L. Prueitt, L. C. Hsieh-Wilson, M. I. Diamond, *J. Biol. Chem.* **2018**, *293*, 10826–10840.
- [5] M. Yamada, T. Hamaguchi, *J. Biol. Chem.* **2018**, *293*, 10841–10842.
- [6] C. I. Gama, S. E. Tully, N. Sotogaku, P. M. Clark, M. Rawat, N. Vaidehi, W. A. G. Iii, A. Nishi, L. C. Hsieh-Wilson, *Nat. Chem. Biol.* **2006**, *2*, 467–473.
- [7] K. C. Güven, K. Akyüz, T. Yurdun, *Toxicol. Environ. Chem.* **1995**, *47*, 65–70.
- [8] T. J. Beveridge, S. F. Koval, *Appl. Environ. Microbiol.* **1981**, *42*, 325–335.
- [9] A. F. Abdulwahid, T. M. Lazim, A. Saat, Z. S. Kareem, *Int. Rev. Autom. Control* **2015**, *8*, 244–250.
- [10] K. J. Waldron, J. C. Rutherford, D. Ford, N. J. Robinson, *Nature* **2009**, *460*, 823–830.
- [11] E.-I. Ochiai, *J. Chem. Educ.* **1995**, *72*, 479.

- [12] D. R. Coombe, W. C. Kett, *Cell. Mol. Life Sci.* **2005**, *62*, 410–424.
- [13] R. F. Parrish, W. R. Fair, *Biochem. J.* **1981**, *193*, 407–410.
- [14] N. S. Gandhi, R. L. Mancera, *Chem. Biol. Drug Des.* **2008**, *72*, 455–482.
- [15] M. Jaishankar, T. Tseten, N. Anbalagan, B. B. Mathew, K. N. Beeregowda, *Toxicology* **2014**, *7*, 60–72.
- [16] P. B. Tchounwou, C. G. Yedjou, A. K. Patlolla, D. J. Sutton, in (Ed.: A. Luch), Springer Basel, Basel, **2012**, pp. 133–164.
- [17] B. Wang, D. Yanli, *Oxid. Med. Cell. Longev.* **2013**, *12*.
- [18] R. A. Bernhoft, *J. Environ. Public Health* **2012**, *10*.
- [19] G. Flora, D. Gupta, A. Tiwari, *Interdiscip. Toxicol.* **2012**, *5*, 47–58.
- [20] V. Uma Devi, *Ecotoxicol. Environ. Saf.* **1996**, *33*, 168–174.
- [21] F. M. El-Demerdash, E. I. Elagamy, *Int. J. Environ. Health Res.* **1999**, *9*, 173–186.
- [22] L. R. Andrade, R. N. Leal, M. Nosedá, M. E. R. Duarte, M. S. Pereira, P. A. S. Mourão, M. Farina, G. M. Amado Filho, *Mar. Pollut. Bull.* **2010**, *60*, 1482–1488.
- [23] G. T. Shen, E. A. Boyle, *Chem. Geol.* **1988**, *67*, 47–62.
- [24] N. Altgård, E. Nilebäck, L. De Battice, I. Pashkuleva, R. L. Reis, J. Becher, S. Möller, M. Schnabelrauch, S. Svedhem, *Acta Biomater.* **2013**, *9*, 8158–8166.
- [25] K. Ajisaka, Y. Oyanagi, T. Miyazaki, Y. Suzuki, *Biosci. Biotechnol. Biochem.* **2016**, *80*, 1179–1185.
- [26] N. Altgård, J. Becher, S. Möller, F. E. Weber, M. Schnabelrauch, S. Svedhem, *J. Colloid Interface Sci.* **2013**, *390*, 258–266.
- [27] M. Delbianco, A. Kononov, A. Poveda, Y. Yu, T. Diercks, J. Jiménez-Barbero, P. H. Seeberger, *J. Am. Chem. Soc.* **2018**, *140*, 5421–5426.
- [28] T. Yamada, R. Sawada, T. Tsuchiya, *Biomaterials* **2008**, *29*, 3503–3513.
- [29] V. Hintze, A. Miron, S. Moeller, M. Schnabelrauch, H. P. Wiesmann, H. Worch, D. Scharnweber, *Acta Biomater.* **2012**, *8*, 2144–2152.
- [30] A. Pichert, S. A. Samsonov, S. Theisgen, L. Thomas, L. Baumann, J. Schiller, A. G. Beck-Sickinger, D. Huster, M. T. Pisabarro, *Glycobiology* **2012**, *22*, 134–145.
- [31] A. K. Picke, J. Salbach-Hirsch, V. Hintze, S. Rother, M. Rauner, C. Kascholke, S. Möller, R. Bernhardt, S. Rammelt, M. T. Pisabarro, G. Ruiz-Gómez, M. Schnabelrauch, M. Schulz-Siegmund, M. C. Hacker, D. Scharnweber, C. Hofbauer, L. C. Hofbauer, *Biomaterials* **2016**, *96*, 11–23.
- [32] L. Koehler, S. Samsonov, S. Rother, S. Vogel, S. Köhling, S. Moeller, M. Schnabelrauch, J. Rademann, U. Hempel, M. T. Pisabarro, D. Scharnweber, V. Hintze, *Sci. Rep.* **2017**, *7*, 1210.
- [33] S. Bhowmick, S. Rother, H. Zimmermann, P. S. Lee, S. Moeller, M. Schnabelrauch, V. Koul, R. Jordan, V. Hintze, D. Scharnweber, *Mater. Sci. Eng. C* **2017**, *79*, 15–22.
- [34] S. Rother, S. A. Samsonov, U. Hempel, S. Vogel, S. Moeller, J. Blaszkiewicz, S. Köhling, M. Schnabelrauch, J. Rademann, M. T. Pisabarro, V. Hintze, D. Scharnweber, *Biomacromolecules* **2016**, *17*, 3252–3261.
- [35] V. Hintze, S. Moeller, M. Schnabelrauch, S. Bierbaum, M. Viola, H. Worch, D. Scharnweber, *Biomacromolecules* **2009**, *10*, 3290–3297.
- [36] D. D. Allison, K. J. Grande-Allen, *Tissue Eng.* **2006**, *12*, 2131–2140.
- [37] N. Afratis, C. Gialeli, D. Nikitovic, T. Tseggenidis, E. Karousou, A. D. Theocharis, M. S. Pavão, G. N. Tzanakakis, N. K. Karamanos, *FEBS J.* **2012**, *279*, 1177–1197.
- [38] U. Hempel, S. Möller, C. Noack, V. Hintze, D. Scharnweber, M. Schnabelrauch, P. Dieter, *Acta Biomater.* **2012**, *8*, 4064–4072.
- [39] J. Necas, L. Bartosikova, P. Brauner, J. Kolar, *Vet. Med.* **2008**, *53*, 397–411.
- [40] S. Rother, S. A. Samsonov, S. Moeller, M. Schnabelrauch, J. Rademann, J. Blaszkiewicz, S. Köhling, J. Waltenberger, M. T. Pisabarro, D. Scharnweber, V. Hintze, *ACS Appl. Mater. Interfaces* **2017**, *9*, 9539–9550.
- [41] S. Köhling, J. Blaszkiewicz, G. Ruiz-Gomez, I. Fernandez-Bachiller, K. Lemmnitzer, N. Panitz, A. G. Beck-Sickinger, J. Schiller, M. Pisabarro, J. Rademann, *Chem. Sci.* **2019**, *10*, 866–878.
- [42] Y. Fujiwara, C. Yamamoto, T. Kaji, *Toxicology* **2000**, *154*, 9–19.
- [43] K. P. Carter, A. M. Young, A. E. Palmer, *Chem. Rev.* **2014**, *114*, 4564–4601.
- [44] K. M. Dean, Y. Qin, A. E. Palmer, *Biochim. Biophys. Acta Mol. Cell Res.* **2012**, *1823*, 1406–1415.
- [45] T. M. Desilva, G. Veglia, F. Porcelli, A. M. Prantner, S. J. Opella, *Biopolymers* **2002**, *64*, 189–197.
- [46] V. N. Uversky, J. Li, A. L. Fink, *J. Biol. Chem.* **2001**, *276*, 44284–44296.
- [47] H. I. Okur, J. Hlad, K. B. Rembert, Y. Cho, J. Heyda, J. Dzubiella, P. S. Cremer, P. Jungwirth, *J. Phys. Chem. B* **2017**, *121*, 1997–2014.
- [48] J. Duguid, V. A. Bloomfield, A. J. Benevides, G. J. Thomas, *Biophys. J.* **1993**, *65*, 1916–1928.
- [49] M. T. Bowers, D. Liu, T. Wyttenbach, *J. Am. Chem. Soc.* **2008**, *130*, 11219.
- [50] E. Snir, J. Joore, P. Timmerman, S. Yitzchaik, *Langmuir* **2011**, *27*, 11212–11221.
- [51] X. Bin, H.-B. Kraatz, *Analyst* **2009**, *134*, 1309–1313.
- [52] E. Mervinetsky, I. Alshanski, Y. Hamo, L. M. Sandonas, A. Dianat, J. Buchwald, R. Gutierrez, G. Cuniberti, M. Hurevich, S. Yitzchaik, *Sci. Rep.* **2017**, *7*, 9498.
- [53] S. D. Keighley, P. Estrela, P. Li, P. Migliorato, *Biosens. Bioelectron.* **2008**, *24*, 906–911.
- [54] J. M. Baskin, J. A. Prescher, S. T. Laughlin, N. J. Agard, P. V. Chang, I. A. Miller, A. Lo, J. A. Codelli, C. R. Bertozzi, *Proc. Natl. Acad. Sci. USA* **2007**, *104*, 16793–16797.
- [55] J. Dommerholt, F. P. J. T. Rutjes, F. L. van Delft, *Top. Curr. Chem.* **2016**, *374*, 1–20.
- [56] I. Jelesarov, H. R. Bosshard, *J. Mol. Recognit.* **1999**, *12*, 3–18.
- [57] W. B. Turnbull, A. H. Daranas, *J. Am. Chem. Soc.* **2003**, *125*, 14859–14866.
- [58] G. Camci-Unal, N. L. B. Pohl, *J. Chem. Eng. Data* **2010**, *55*, 1117–1121.
- [59] S. Köhling, G. Künze, K. Lemmnitzer, M. Bermudez, G. Wolber, J. Schiller, D. Huster, J. Rademann, *Chem. Eur. J.* **2016**, *22*, 5563–5574.
- [60] S. Köhling, M. P. Exner, S. Nojoui, J. Schiller, N. Budisa, J. Rademann, *Angew. Chem. Int. Ed.* **2016**, *55*, 15510–15514; *Angew. Chem.* **2016**, *128*, 15736–15740.
- [61] H. I. Yoon, J. Y. Yhee, J. H. Na, S. Lee, H. Lee, S. W. Kang, H. Chang, J. H. Ryu, S. Lee, I. C. Kwon, Y. Woo Cho, K. Kim, *Bioconjugate Chem.* **2016**, *27*, 927–936.
- [62] K. K. Tadi, I. Alshanski, E. Mervinetsky, G. Marx, P. Petrou, K. M. Dimitrios, C. Gilon, M. Hurevich, S. Yitzchaik, *ACS Omega* **2017**, *2*, 8770–8778.
- [63] A. Gankin, E. Mervinetsky, I. Alshanski, J. Buchwald, A. Dianat, R. Gutierrez, G. Cuniberti, R. Sfez, S. Yitzchaik, *Langmuir* **2019**, *35*, 2997–3004.
- [64] A. Gankin, R. Sfez, E. Mervinetsky, J. Buchwald, A. Dianat, L. Medrano Sandonas, R. Gutierrez, G. Cuniberti, S. Yitzchaik, *ACS Appl. Mater. Interfaces* **2017**, *9*, 44873–44879.
- [65] H. L. M. van Gaal, J. G. M. van der Linden, *Coord. Chem. Rev.* **1982**, *47*, 41–54.
- [66] L. Mercier, T. J. Pinnavaia, *Environ. Sci. Technol.* **1998**, *32*, 2749–2754.
- [67] J. A. Cowan, *Chem. Rev.* **1998**, *98*, 1067–1088.
- [68] A. G. Gerbst, V. B. Krylov, D. A. Argunov, M. I. Petruk, A. S. Solovov, A. S. Dmitrenok, N. E. Nifantiev, *Beilstein J. Org. Chem.* **2019**, *15*, 685–694.
- [69] T. Maruyama, T. Toida, T. Imanari, G. Yu, R. J. Linhardt, *Carbohydr. Res.* **1998**, *306*, 35–43.

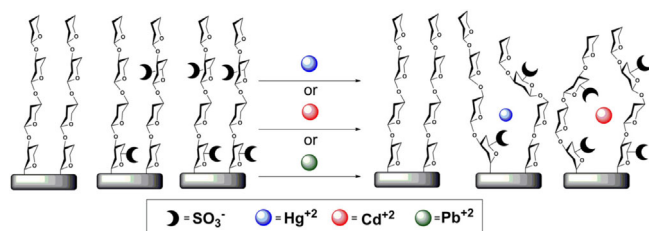
Manuscript received: April 2, 2019

Revised manuscript received: May 30, 2019

Accepted manuscript online: June 2, 2019

Version of record online: ■■■ 0000

## FULL PAPER



**Pattern recognition:** The effect of sulfation patterns on the metal binding properties of saccharides is enigmatic because the accessibility to structurally defined sulfated saccharides is limited and because of the absence of suitable

analytical techniques. Herein, electrochemical methods are used to show that the sulfation pattern of hyaluronic acid governs their heavy metal ions binding preferences (see scheme).

### Carbohydrates

*I. Alshanski, J. Blaszkiewicz,  
E. Mervinetsky, J. Rademann,\*  
S. Yitzchaik,\* M. Hurevich\**



### Sulfation Patterns of Saccharides and Heavy Metal Ion Binding

